Tectonophysics 584 (2013) 138–143

Contents lists available at SciVerse ScienceDirect

Tectonophysics

journal homepage: www.elsevier.com/locate/tecto

Inter-seismic deformation field of the Ganzi-Yushu fault before the 2010 Mw 6.9 Yushu earthquake

Yanzhao Wang [a], Min Wang [a], Zheng-Kang Shen [b,*], Weipeng Ge [a], Kang Wang [b], Fan Wang [a], Jianbao Sun [a]

[a] State Key Laboratory of Earthquake Dynamics, Institute of Geology, China Earthquake Administration, Beijing 100029, China
[b] School of Earth and Space Science, Peking University, Beijing 100871, China

ARTICLE INFO

Article history:
Received 31 August 2011
Received in revised form 11 January 2012
Accepted 23 March 2012
Available online 3 April 2012

Keywords:
Yushu earthquake
Ganzi-Yushu fault
GPS
Fault slip rate

ABSTRACT

The 14 April 2010 Mw 6.9 Yushu earthquake ruptured the northwestern segment of the Ganzi-Yushu fault in Qinghai Province, China. Using GPS data obtained from 1999 to 2007 in the vicinity of the Ganzi-Yushu fault, we estimate the slip rates of the Fenghuoshan and Ganzi-Yushu faults, and the northwestern segment of the Xianshuihe fault as 6.1 ± 1.9, 6.6 ± 1.5, and 9.7 ± 0.7 mm/a for left lateral components, and 2.8 ± 1.9, 1.7 ± 1.6, and -2.0 ± 0.9 mm/a for shortening components, respectively. The Maduo-Gande fault slips left laterally at a rate of about 1–2 mm/a, and ~3 mm/a sinistral shear motion is left unexplained, possibly caused by deformation across one or more unknown faults in the region. These results agree with geological estimates of the fault slip rates, and show a progressive increase of shear motion from northwest to southeast across segments of the Xianshuihe–Ganzi-Yushu fault zone, implying variation in transferring and absorbing deformation in different regions in and around the Tibetan plateau.

1. Introduction

The 14 April 2010 Mw 6.9 Yushu earthquake ruptured the northwestern segment of the Ganzi-Yushu fault (Chen et al., 2010) (Fig. 1). This fault belongs to the Xianshuihe–Ganzi-Yushu fault system, whose left-lateral slip, as part of the eastward extrusion process, transports the crustal materials of the southeast borderland of the Tibetan plateau east–southeastward and out of the plateau (Wang et al., 2008a). Three strong earthquakes were recorded along the northwestern segment of the Ganzi-Yushu fault in the last two centuries, of which the 1738 M 6.5 Yushu earthquake ruptured approximately the same segment of the 2010 Yushu earthquake (Institute of Geophysics, China Seismological Bureau, 1990), and the other two events occurred to the east of Yushu (Earthquake Forecasting Division of Center for Earthquake Monitoring and Forecast, China Seismological Bureau, 1999; Editorial Group of the Data Compilation of Earthquakes in Sichuan, 1980). Studies using teleseismic data revealed a primarily left-lateral slip mechanism of the 2010 Yushu earthquake, with the hypocenter located ~40 km west–northwest of Yushu at a depth of ~17 km (http://earthquake.usgs.gov/earthquakes/eqinthenews/2010/us2010vacp/). Field investigations discovered surface breaks of the fault about 80 km long, with the maximum horizontal offset of ~1.8 m located ~15 km west of Yushu (Chen et al., 2010).

Significant progress has been made in recent years about understanding tectonic deformation of the Ganzi-Yushu fault (Institute of Geophysics, China Seismological Bureau, 1990; Li et al., 1995; Peng et al., 2006; Wen et al., 2003; Zhang et al., 1996; Zhou et al., 1996; see Fig. 2 for summary). Nevertheless, debates still exist on the displacements and the slip rates across different segments of the fault. Li et al. (1995) revealed a left lateral slip rate of 7.3 mm/a across the segment west of Longmengda since Holocene. They also claimed primarily normal slip before the late Pleistocene and no evidence of Holocene activity across the Longmengda-Yushu segment of the fault. In contrast, the 1738 Yushu earthquake implies contemporary left-lateral slip across the segment (Institute of Geophysics, China Seismological Bureau, 1990). The slip rate of the Yushu-Zhuqing segment was estimated as ~5 mm/a over the Holocene (Li et al., 1995). A left-lateral slip rate of 7.3 mm/a, averaged over the past 14 thousand years, was also inferred across the Dangjiang segment (Zhang et al., 1996). Zhou et al. (1996) obtained average slip rates of 7.0 ± 0.7 mm/a and 7.2 ± 1.2 mm/a across the Cuoa-Ezhi and Dangtuo segments, respectively. Quite different slip rate results were deduced by Peng et al. (2006), with 5.4 ± 0.4 and 3.3 ± 0.3 mm/a at the Ezhi and Zhuqing segments, respectively, which is perhaps less reliable, since the inception time of the fault was crudely inferred rather than determined by any dating method. Wen et al. (2003) estimated the average slip rate at Dangtuo in Holocene as 11.3 ± 1.8 mm/a (Wen et al., 2003). But this result might be an overestimation, since they assumed that the inception time of left lateral slip faulting was closer to the age of the terrace below the offset terrace risers, which should only be the lower bound of the inception time; and older inception time would mean lower estimate on fault slip rate.

* Corresponding author. Tel.: +86 10 62754037.
E-mail address: zhengkangshen@pku.edu.cn (Z.-K. Shen).

0040-1951/$ – see front matter © 2012 Elsevier B.V. All rights reserved.
doi:10.1016/j.tecto.2012.03.026

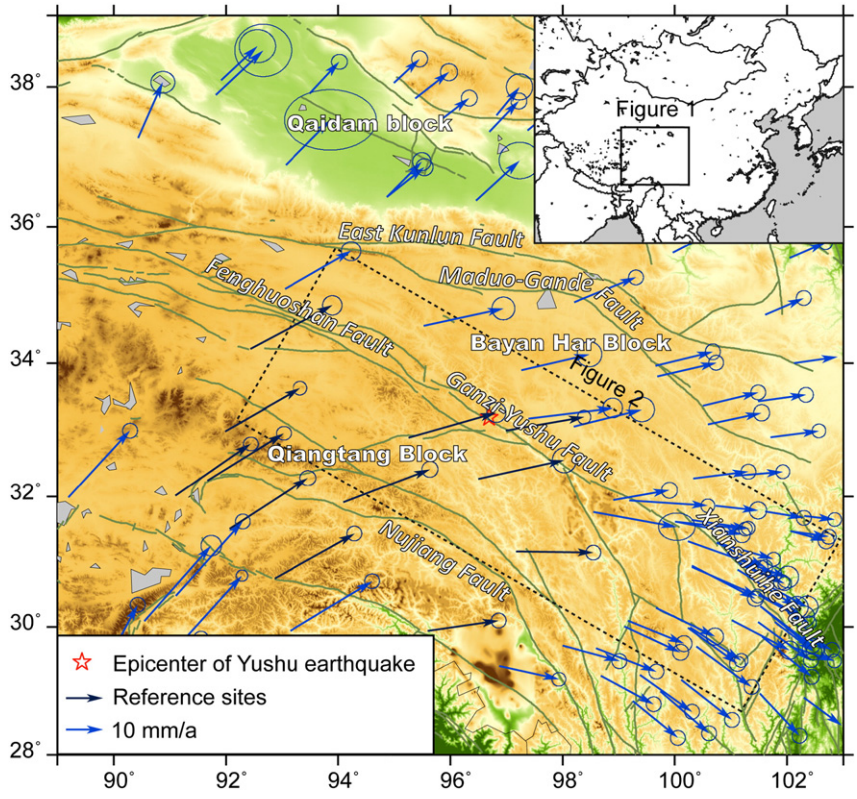

Fig. 1. Tectonic setting and GPS derived horizontal velocity field of the studied region. The red star is the epicenter of the 2010 Yushu earthquake. The arrows are GPS velocities with respect to the Eurasia plate, with the error ellipses representing 70% confidence. The dark blue arrows are GPS velocities used to calculate the Euler vector of the eastern Qiangtang block.

During the last two decades, GPS data have been collected and used to deduce present day crustal deformation field in and around the Tibetan plateau. Wang et al. (2001) summarized GPS measurements made prior to 2000 and produced a set of solution for continental China. Subsequent studies, using GPS data mainly from the Crustal Motion Observation Network of China (CMONC) project, produced solutions with more data epochs included at later times (Gan et al., 2007; Niu et al., 2005; Wang et al., 2003; Zhang et al., 2004).

The present-day slip rate of the Ganzi-Yushu fault has been estimated based on these velocity data (Fig. 2). Meade (2007) devised a block motion model and inferred a slip rate of 9–12 mm/a across the fault, which is consistent with that reported by Thatcher (2007) (~11 mm/a) obtained also using a block motion model. Gan et al. (2007), on the other hand, found a larger rate of ~14.4 mm/a. A recent update by Loveless and Meade (2011) also placed 10.2 ± 0.2–14.6 ± 0.3 mm/a left lateral slip on this segment of the fault. These results are much larger than most of the geologic estimates, which we attribute to their assumption of undeformed blocks on either side of the Xianshuihe–Ganzi-Yushu fault or a single slip rate rather than spatially varying slip rates along the fault. Specifically, since both Meade (2007) and Thatcher (2007) treated the Ganzi-Yushu and Xianshuihe faults as the boundaries between the same two blocks, slip rate estimates across the two faults are then tied together to the relative block motion rate, and therefore are heavily manifested by relative motion rates across the Xianshuihe fault since GPS station density is much higher across the Xianshuihe fault than across the Ganzi-Yushu fault. Though more GPS data were added in the model in Gan et al. (2007), the Xianshuihe–Ganzi-Yushu fault was assumed to have a single slip rate, thus the high slip rate of the Xianshuihe fault around which densely distributed GPS data must result in an overestimation of the slip rate across the Ganzi-Yushu fault. Wang et al. (2008b) used a more detailed model and detected slip rates of 13.0 ± 1.7 and 3.1 ± 2.8 mm/a across the southeastern and northwestern segments of the Ganzi-Yushu fault. Unfortunately, the Ganzi-Yushu fault is located at the northwestern corner of the studied region, and lacking data further to the west for more complete coverage resulted in a less reliable estimate of the fault slip rates.

In this study we collect more GPS data around the Ganzi-Yushu fault to determine the inter-seismic horizontal velocity field. Better estimation of the contemporary slip rates along segments of the Xianshuihe–Ganzi-Yushu fault will be helpful in improving the understanding of the seismo-tectonics of the fault and evolution of the earthquake processes.

2. GPS data and analysis

GPS data used in this study are mainly from the Crustal Motion Observation Network of China (CMONC) project, including data observed on survey mode sites in 1999, 2001, 2004, and 2007. We also include data observed at the geodetic control points by the Military Bureau of Surveying and Mapping and the State Bureau of Surveying and Mapping during the same time period and a few years earlier. Combined with GPS data from global IGS tracking stations, these data were processed to obtain station positions and velocities with respect to a global reference frame (Wang, 2009). Although we have collected almost all the GPS data in this region, spatial coverage of these observations are still not dense enough for reliable estimates of kinematic parameters of a block motion model. We therefore choose the profile projection approach to examine the deformation field of this region. In order to accentuate the difference in crustal motion across the Ganzi-Yushu fault, velocities of 12 GPS stations within the eastern Qiangtang block were used to calculate its Euler vector (Fig. 1), and the corresponding velocity field with respect to the eastern Qiangtang block was obtained by removing the rigid block motion from the horizontal velocity field (Fig. 3). This process is

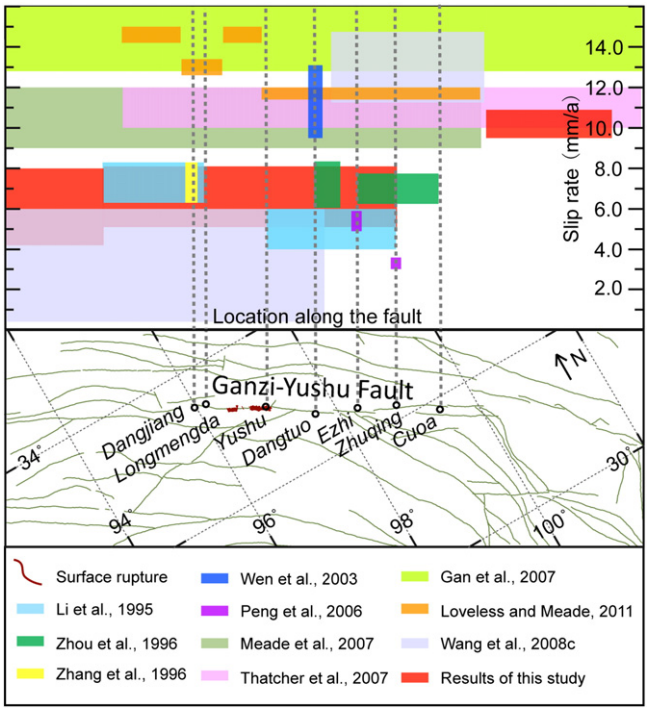

Fig. 2. Slip rate estimations across segments of the Xianshuihe–Ganzi-Yushu fault. Dark red lines show the surface rupture of the 2010 Yushu earthquake. Light blue, dark green, yellow, dark blue, and purple bars show extent and location of the fault segments and the estimated slip rates from geological studies by Li et al. (1995), Zhou et al. (1996), Zhang et al. (1996), Wen et al. (2003), and Peng et al. (2006), respectively. Sage green, pink, grass green, orange, and gray bars show extent of fault segments and the estimated slip rates from geodetic studies by Meade (2007), Thatcher (2007), Gan et al. (2007), Loveless and Meade (2011), and Wang et al. (2008b) respectively. The red bars show our results.

important in defining a reference frame, from which we will be able to separate both the shear and normal deformation across the fault from the rigid rotation of the regional block. The reason for not choosing the Bayan Har block north of the Ganzi-Yushu fault as the reference frame is that the Bayan Har block is a narrow strip located between the Maduo-Gande and Ganzi-Yushu faults, and within the region the GPS velocity data points are limited and scattered, making it difficult to reliably resolve a rigid block motion model.

To study fault slip rates across the Xianshuihe–Ganzi-Yushu fault system we select three GPS velocity profiles across the Fenghuoshan and Ganzi-Yushu faults, and the northwestern segment of the Xianshuihe fault (Fig. 3). GPS station velocities within three rectangles spanning the three fault segments are decomposed into strike-parallel and strike-normal components respectively, as shown in Fig. 3. The velocity profiles indicate deformation across not only the Xianshuihe–Ganzi-Yushu fault but also the Nujiang, East Kunlun, and Maduo-Gande faults. Detailed studies about the fault structure and locking are difficult, because the data are somewhat scattered, and there are not enough near-field observations to constrain the deformation gradient across the fault associated with the fault locking effect. We therefore eliminate the near-field data affected by fault locking and far-field data affected by activities of other faults, and focus on the remaining intermediate- and far-field data for estimation of gross deformation across the fault segments. The stations whose velocities are used to estimate fault slip rates across the Fenghuoshan, Ganzi-Yushu, and Xianshuihe faults are approximately more than 50, 70, and 60 km away from the faults. The elastic deformation due to fault locking will bias the station velocities by at most 12%, 9%, and 10% of the total fault slip rates for a locking depth of 20 km, or 9%, 7%, and 8% for a locking depth of 15 km respectively according to Savage and Burford (1973). For example, even if the fault slip rate is 8 mm/a, the station velocities will not be biased by more than 1 mm/a. Also, since the adjacent faults are located more than 100 km away from the Xianshuihe–Ganzi-Yushu fault, biases of

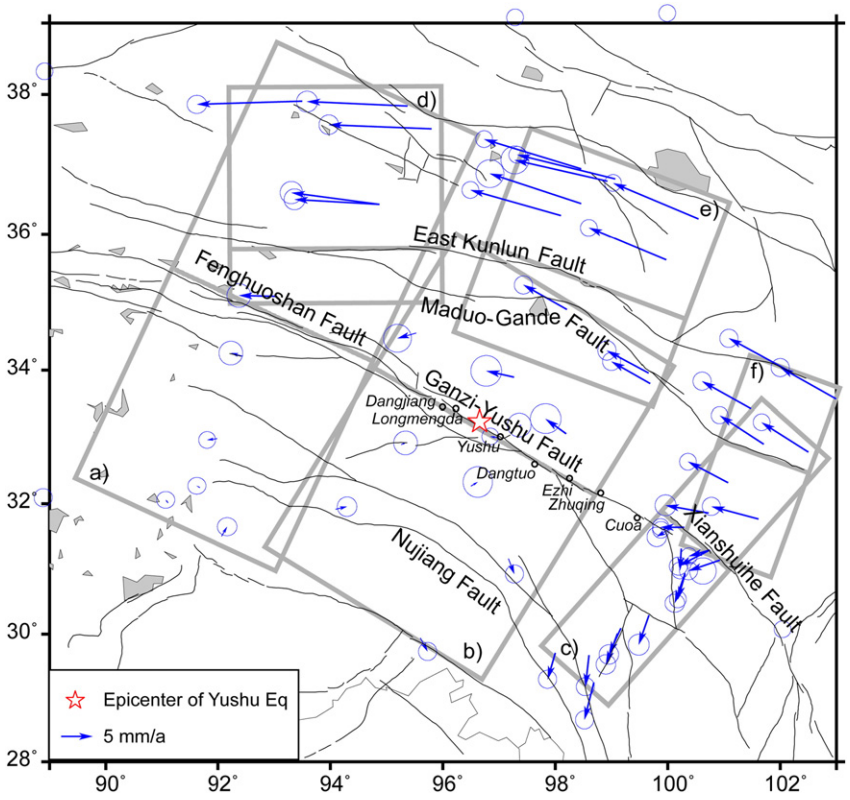

Fig. 3. GPS velocity field with respect to the eastern Qiangtang block, with the error ellipses representing 70% of confidence. The gray rectangular frames encompassing fault segments mark the regions within which stations are depicted for slip rate estimation and their velocity profiles are shown in Fig. 4.

station velocities due to elastic deformation associated with these faults are no more than 6% of their slip rates, i.e., 0.5–0.8 mm/a for slip rates of 8–12 mm/a with fault locking depth of 20 km.

Therefore, we ignore the elastic deformation due to fault locking, and the strike-slip and normal components of slip rate across each fault segment is estimated as the difference between the weighted mean values of the strike-parallel and normal components of the station velocities on either side of the fault. At the same time, uncertainties of slip rates are also obtained through propagating formal uncertainties of GPS velocities. Since data used in this study were originally referenced to the fiducial sites located in northern Europe and Siberia during GPS velocity estimation, the formal uncertainties of the velocities would be overestimated by ~50% than if the solution was referenced locally. Also, the velocities are correlated locally at 50–70% for neighboring sites, thus the amount of under-estimation of the uncertainties of fault slip rates by ignoring these correlations, roughly speaking, could be 20–50%. The overall effect to our conclusions due to these over- and under-estimation of uncertainties therefore, as we believe, will not be significant. Accordingly, the left lateral slip rates of the Fenghuoshan and Ganzi-Yushu faults, and the northwestern segment of the Xianshuihe fault are estimated as 6.1 ± 1.9, 6.6 ± 1.5, and 9.7 ± 0.7 mm/a, respectively. And the normal slip rates are also determined as 2.8 ± 1.9 and 1.7 ± 1.6 mm/a shortening across the Fenghuoshan and Ganzi-Yushu faults, and 2.0 ± 0.9 mm/a extension across the northwestern segment of the Xianshuihe fault, respectively. These results represent the total slip rates across each segment of the fault zone, which might include contributions from secondary faults in the region.

Our estimation of the left lateral slip rate across the Ganzi-Yushu fault is consistent with geological results obtained from investigation of landform offset and geochronologic dating (Li et al., 1995; Zhang et al., 1996; Zhou et al., 1996), but disagrees with those derived by Meade (2007), Thatcher (2007), Gan et al. (2007), and Loveless and Meade (2011) using GPS data. As we mentioned earlier, these geodetic results might be overestimations due to the higher slip rate along the Xianshuihe fault and the assumption of rigid block motions on both sides of the fault. Wang et al.'s (2008b) estimates of fault slip rates suffer from large uncertainties. Nevertheless they still support lower slip rates across the Ganzi-Yushu fault within the error. In conclusion, GPS determined present-day slip rates of the Fenghuoshan and Ganzi-Yushu faults are consistent with geologically determined fault slip rates averaged in Holocene time, and both fault segments slipped at rates lower than that of the Xianshuihe fault.

In addition, we estimate the slip rates across the western and central segments of the East Kunlun fault and the eastern segment of the Maduo-Gande fault using GPS station velocities with respect to the Qaidam block in the north. As shown in Figs. 3 and 4, there is no GPS station located between the East Kunlun and Maduo-Gande faults except near the east end of the Maduo-Gande fault, and there are only a couple of near-field sites and no intermediate sites on the southern side of the Maduo-Gande fault. Therefore, we could only obtain a total slip rate across both faults for the central and western segments, and most of the slip is likely to come from the East Kunlun fault. Our results show 8.9 ± 1.0 and 6.7 ± 0.6 mm/a left lateral slip and 2.3 ± 1.6 and 0.9 ± 0.6 mm/a shortening across the western and central segments of the East Kunlun and Maduo-Gande faults,

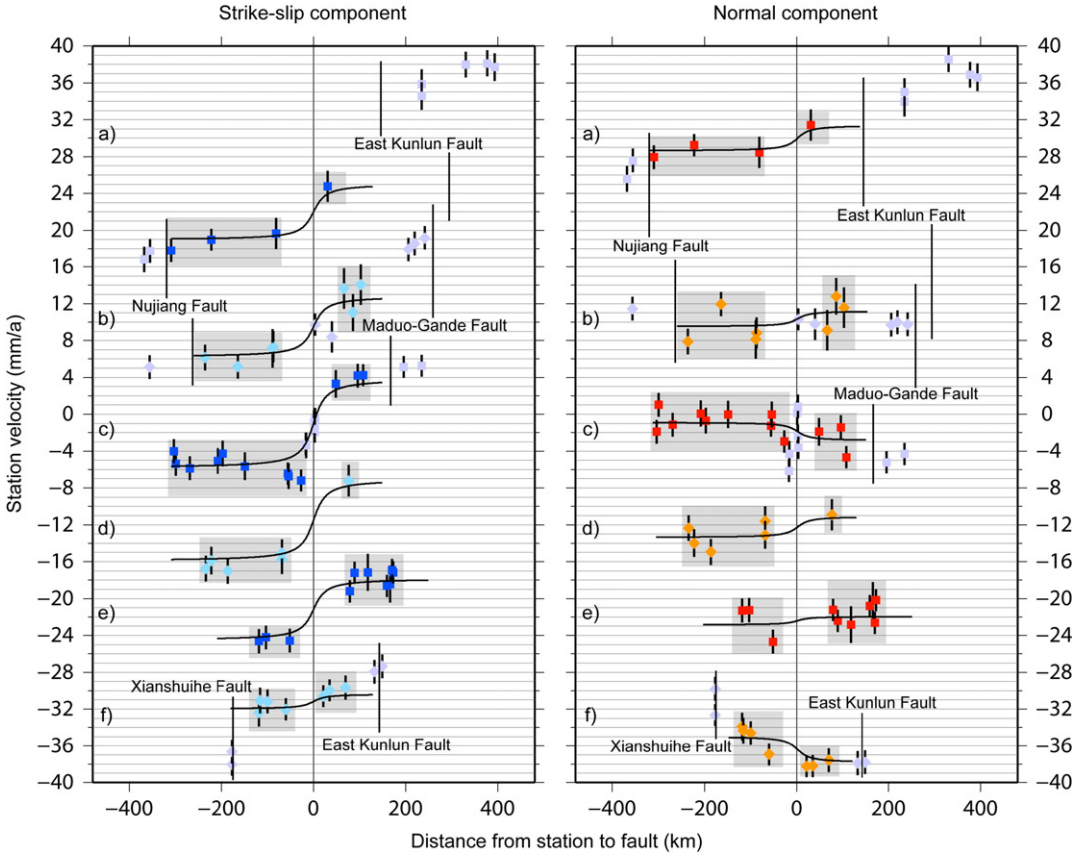

Fig. 4. Velocity profiles across fault segments. The left and right panels show GPS velocity components parallel (sinistral positive) and perpendicular (compressional positive) to the strike of the fault, respectively. Blue and red squares and light blue and orange diamonds represent data used for calculating the fault slip rates, and the gray squares/diamonds are those eliminated from the calculation due to contamination by fault locking effect and/or activities of other faults. Black curves show the predicted displacements across fault segments with estimated fault slip rates and fault locking depth of 20 km.

respectively. Two stations located more than 100 km south of the Maduo-Gande fault show more eastward motion than the sites closer to the fault, and such a velocity difference cannot be explained by elastic deformation due to locking of the East Kunlun and Maduo-Gande faults (Fig. 4). These two sites are therefore excluded from slip rate estimate of the two faults. The slip rate estimates given above are a bit lower than most of the geologic estimates (11 ± 2 mm/a from Van der Woerd et al., 1998, 2000, 2002; 10 ± 1.5 mm/a from Li et al., 2005) and that derived using GPS data (~10 mm/a from Meade, 2007 and 10.5 mm/a from Loveless and Meade, 2011), but consistent with most of the geodetic ones (6–7 mm/a from Thatcher, 2007; 7.1 ± 1.4 mm/a from Wang et al., 2008b; 8–12 mm/a from Kirby et al., 2007).

The eastern segment of the Maduo-Gande fault is estimated to undergo 1.6 ± 0.4 mm/a sinistral slip and 2.9 ± 0.8 mm/a shortening, which contribute to the velocity gradient in the region north of the Xianshuihe fault. According to our estimates and results of previous studies, we infer that the slip rate across the Maduo-Gande fault must be low, at the level of 1–2 mm/a. We also notice that the velocity difference between the Maduo-Gande and Ganzi-Yushu faults is as large as ~7 mm/a over a distance of ~150 km, which could not be interpreted entirely by the elastic deformation due to left lateral slip across the two faults. Taking ~7 mm/a and 1–2 mm/a slip rates across the Ganzi-Yushu and Maduo-Gande faults, contributions from elastic deformation of the two faults are ~3 and ~1 mm/a for velocity difference over a distance of 150 km. Therefore there might be one or more active faults located in the region, with a total left lateral slip rate of ~3 mm/a. For the Nujiang fault located south of the Ganzi-Yushu fault, it is difficult to obtain a reliable estimation of slip rate, since the station coverage south of the fault is quite sparse. The limited dataset in the region seems to suggest around 1–3 mm/a sinistral slip across the fault.

Fig. 4 also shows an uneven distribution of velocity profile across the Xianshuihe fault, which is likely due to the complex deformation pattern in the region south of the fault. Velocities of three sites located 30–60 km southwest of the Xianshuihe fault might have been contaminated by dextral shear deformation associated with one or more minor faults located west of these stations.

3. Discussion and conclusions

Using GPS data obtained from 1999 to 2007, we have determined that the Fenghuoshan and Ganzi-Yushu faults, and the northwestern segment of the Xianshuihe fault slip left-laterally at rates of 6.1 ± 1.9, 6.6 ± 1.5, and 9.7 ± 0.7 mm/a, respectively. The shortening rates across the Fenghuoshan and Ganzi-Yushu faults are 2.8 ± 1.9 and 1.7 ± 1.6 mm/a, respectively, and the extensional rate across the northwestern segment of the Xianshuihe fault is 2.0 ± 0.9 mm/a. We have also found that the net left lateral slip rate across the western and central segments of the East Kunlun and Maduo-Gande faults is ~8 mm/a. These results agree with most of the previous geological studies. About 3 mm/a sinistral shear motion is also detected between the Ganzi-Yushu and Maduo-Gande faults, suggesting faulting on unknown faults in the region.

The last strong earthquake that struck Yushu on the Ganzi-Yushu fault was in 1738, which was 272 years prior to the 2010 earthquake (Institute of Geophysics, China Seismological Bureau, 1990). If the fault slip rate during this time period was 6.6 mm/a, the same as what we obtained in this study, the accumulated slip deficit on fault would be ~1.8 m, incidentally equal to the maximum surface rupture of the 2010 event (Chen et al., 2010). Such an agreement may be more than just a coincidence.

Our studies indicate progressive increase of left lateral slip from northwest to southeast along the Xianshuihe–Ganzi-Yushu fault, with a thrust component across the Ganzi-Yushu fault and an extensional component across the Xianshuihe fault, respectively. This finding agrees with geologically determined variation of slip along the fault since early Pleistocene (Wang et al., 2008a). By measuring the landform offsets, Wang et al. (2008a) detected sinistral displacements of ~16 and ~25 km across the Yushu fault at Dangjiang and Yushu, respectively. Such a differential slip between the two spots is supposed to be absorbed by extensional slip across the Batang and Xialaxiu faults to the south and shortening deformation within the Yushu block to the north. This also explains the discrepancy between fault slip rates estimated previously by geodetic models and most of geological studies, as the geodetic models assumed undeformed blocks on either side of the Xianshuihe–Ganzi-Yushu fault, allowing no spatial variation of slip rate along the fault.

The deformation pattern varies remarkably across the Tibetan plateau. A cluster of northeast- and northwest-trending conjugate shear faults exist in central and western Tibetan plateau, connecting a group of N–S trending rifts in southern Tibet (Armijo et al., 1986; Yin and Harrison, 2000). The N–S shortening resulted from Indo-Asia collision is therefore accommodated by sinistral slip on the northeast-trending and dextral slip on the northwest-trending conjugate faults in the Qiangtang terrane in central and western Tibet, and the squeezed materials are extruded eastward during this process. As more crustal materials are extruded from west to east, differential shear across the shear zone north of the Qiangtang block is also increasing (Shen et al., 2003; Zhang et al., 2004). As a result, the conjugate shear faults and rifts are replaced by large strike-slip faults, such as the Xianshuihe–Ganzi-Yushu and East Kunlun faults, as left lateral faulting becomes the most effective means of moving material out of the eastern plateau. In this process, the two faults act as steps of material movement from south to north, and the increase of slip rates along the Xianshuihe–Ganzi-Yushu fault transports materials progressively from west to east. Since the strike of the Ganzi-Yushu fault bends gradually to the south from west to east, the eastward movement of materials south of the fault must be imposing a slight amount of thrust motion across the fault. On the contrary, however, due to rapid decrease of surface elevation in the region southwest of the Xianshuihe fault from north to south, the gravitational collapse would speed up the southward escape of this region, resulting in reduced or even no thrust motion across the northwestern segment of the Xianshuihe fault.

Following the 2010 Yushu earthquake, in order to monitor the postseismic deformation of the seismogenic Ganzi-Yushu fault and its surroundings, we occupied 6 continuous GPS stations in a profile across the fault at the Yushu-Jiegu town. The observations will provide data for research on the rheological structure of the fault zone and the surrounding crust, as well as their response to the earthquake. The secular fault slip rates estimated in this study provides crucial constraints on background and initial deformation field for postseismic deformation modeling studies in the future.

Acknowledgments

We thank Lichun Chen for providing the rupture data of the 2010 Yushu earthquake. We are also grateful to Honglin He, Jeff Freymueller, and an anonymous reviewer for helpful comments. This work was supported by the State Key Laboratory of Earthquake Dynamics (LED2009A02 and LED2008A05), the Fundamental Research Funds for the Institute of Geology, China Earthquake Administration (IGCEA1011), and the Natural Science Foundation of China (41090294).

References

Armijo, R., Tapponnier, P., Mercier, J.L., et al., 1986. Quaternary extension in southern Tibet: field observations and tectonic implications. Journal of Geophysical Research 91 (B14), 13803–13872.

Chen, L., Wang, H., Ran, Y., et al., 2010. The Ms7.1 Yushu earthquake surface ruptures and historical earthquakes. Chinese Science Bulletin 55. doi:10.1007/s11434-010-0293-1.

Earthquake Forecasting Division of Center for Earthquake Monitoring and Forecast, China Seismological Bureau, 1999. The catalogue of strong earthquakes in China (from 23 century B.C. to 1999 A. D.).
Editorial Group of the Data Compilation of Earthquakes in Sichuan, 1980. The Data Compilation of Earthquakes in Sichuan (Book 1). People's Publishing House of Sichuan, Chengdu, pp. 1–576.
Gan, W., Zang, P., Shen, Z., et al., 2007. Present-day crustal motion within the Tibetan Plateau inferred from GPS measurements. Journal of Geophysical Research 112, B08416. doi:10.1029/2005JB004120.
Institute of Geophysics, China Seismological Bureau, 1990. Atlas of Historical Earthquakes in China, the Qing Dynasty Period. SinoMaps Press, Beijing, p. 24.
Kirby, E., Harkins, N., Wang, E., et al., 2007. Slip rate gradients along the eastern Kunlun fault. Tectonics 26. doi:10.1029/2006TC002033.
Li, M., Xing, C., Cai, C., et al., 1995. Research on activity of Yushu fault. Seismology and Geology 17, 218–224.
Li, H., Van der Woerd, J., Tapponnier, P., et al., 2005. Slip rate on the Kunlun fault at Hongshui Gou, and recurrence time of great events comparable to the 14/11/2001, Mw 7.9 Kokoxili earthquake. Earth and Planetary Science Letters 237, 285–299.
Loveless, J.P., Meade, B.J., 2011. Partitioning of localized and diffuse deformation in the Tibetan Plateau from joint inversions of geologic and geodetic observations. Earth and Planetary Science Letters 303, 11–24.
Meade, B., 2007. Present-day kinematics at the India–Asia collision zone. Geology 35 (1), 81–84.
Niu, Z., Wang, M., Sun, H., et al., 2005. Contemporary velocity field of crustal movement of Chinese mainland from Global Positioning System measurements. Chinese Science Bulletin 50 (8), 839–840.
Peng, H., Ma, X., Bai, J., et al., 2006. Characteristics of Quaternary activities of the Garzê-Yushu fault zone. Journal of Geomechanics 12 (3), 295–304.
Savage, J.C., Burford, R.O., 1973. Geodetic determination of relative plate motion in central California. Journal of Geophysical Research 78, 832–845.
Shen, Z., Wang, M., Gan, W., et al., 2003. Contemporary tectonics strain rate field of Chinese continent and its geodynamic implication. Earth Science Frontiers 10(s), 93–100.
Thatcher, W., 2007. Microplate model for the present-day deformation of Tibet. Journal of Geophysical Research 112, B01401. doi:10.1029/2005JB004244.
Van der Woerd, J., Ryerson, F., Tapponnier, P., et al., 1998. Holocene left-slip rate determined by cosmogenic surface dating on the Xidatan segment of the Kunlun Fault (Qinghai, China). Geology 26, 695–698.
Van der Woerd, J., Ryerson, F., Tapponnier, P., et al., 2000. Uniform slip-rate along the Kunlun Fault: implications for seismic behavior and large-scale tectonics. Geophysical Research Letters 27, 2353–2356.
Van der Woerd, J., Tapponnier, P., Ryerson, F., et al., 2002. Uniform postglacial slip-rate along the central 600 km of the Kunlun Fault (Tibet), from ^{26}Al, ^{10}Be, and ^{14}C dating of riser offsets, and climatic origin of the regional morphology. Geophysical Journal International 148, 356–388.
Wang M., 2009. Analysis of GPS data with high precision and study on present-day crustal deformation in China. Doctoral dissertation of Institute of Geology, CEA.
Wang, Q., Zhang, P., Freymueller, J., et al., 2001. Present-day crustal deformation in China constrained by Global Positioning System measurements. Science 294, 574–577.
Wang, M., Shen, Z., Niu, Z., et al., 2003. Contemporary crustal deformation of the Chinese continent an tectonic block model. Science in China Series D 33(s), 21–32.
Wang, S., Fan, C., Wang, G., et al., 2008a. Late Cenozoic deformation along the northwestern continuation of the Xianshuihe fault system, Eastern Tibetan Plateau. GSA Bulletin 120 (3/4), 312–327.
Wang, Y., Wang, E., Shen, Z., et al., 2008b. GPS-constrained inversion of present-day slip rates along major faults of the Sichuan-Yunnan region, China. Science in China Series D 51 (9), 1267–1283.
Wen, X., Xu, X., Zheng, R., et al., 2003. Average slip-rate and recent larth earthquake ruptures along the Ganzi-Yushu fault. Science in China Series D 33(s), 199–208.
Yin, A., Harrison, T.M., 2000. Geological evolution of the Himalayan-Tibetan orogen. Annual Review of Earth and Planet Science 28, 211–280.
Zhang, Y., Li, M., Meng, Y., et al., 1996. Research on fault activity in the Bayan Har Mountain region and the seismic and geologic implications. Research on Active Faults 5, 154–171.
Zhang, P., Shen, Z., Wang, M., et al., 2004. Continuous deformation of the Tibetan Plateau from global positioning system data. Geology 32 (9), 809–812.
Zhou, R., Ma, S., Cai, C., 1996. Late Quaternary active feature of the Ganzi-Yushu fault zone. Earthquake Research in China 12 (3), 250–260.